JOURNAL OF PROPULSION AND POWER
Vol. 21, No. 2, March–April 2005

Spheromak Fusion Propulsion for Future Solar-System Exploration

T. R. Jarboe,* K. M. Parker,† T. A. Mattick,* M. M. Craw,† P. Gu,† W. T. Hamp,† A. A. Hwang,† V. A. Izzo,† P. D. Jewell,† H. Kim,† P. A. Melnik,† P. E. Sieck,† T. Takeda,† and C. T. Tran†
University of Washington, Seattle, Washington 98185

Fusion propulsion for the exploration of the solar system is investigated. Minimum round-trip times for missions to Europa and Mars are given as a function of power/mass ratio. A preconceptual study of a spheromak-based, deuterium burning, fusion propulsion system is presented. The spheromak is sustained by inductive helicity injection with the diverted edge plasma becoming the rocket exhaust. Power/mass ratios of nearly 2 kW/kg appear possible, giving round-trip times of about 100 day for Mars and about one year for Europa. The vessel mass is 540 t not including fuel, a size suitable for human living. The I_{SP} is optimized for a trip to Europa and a trip to Mars and was found to vary between 10,000 to 40,000 s.

Nomenclature

a	=	acceleration
$\boldsymbol{B}$	=	magnetic field
c_e	=	exhaust speed
c_{ex}	=	minimum exhaust speed
$\boldsymbol{E}$	=	electric field
e	=	magnitude of electron charge
I_{SP}	=	specific impulse
$\boldsymbol{j}$	=	electrical current density
L_{rctr}	=	reactor length
m	=	particle mass
$\dot{m}$	=	mass flow rate
m_{elc}	=	mass of all electrical power equipment
m_f	=	final mass
m_0	=	initial mass of rocket and fuel
n	=	particle density
P	=	power into the exhaust
P_{brem}	=	bremsstrahlung radiation
P_n	=	pressure at point n on Fig. 8
P_{syn}	=	synchrotron radiation
p	=	pressure
Q	=	power out/power in or heat flux
R_e	=	radius of Earth's orbit around the sun
r	=	radius
r_{gi}	=	radius of ion gyro radius
r_p	=	pressure ratio
S	=	safety factor
T	=	temperature or sometimes tritium
T_e	=	electron temperature
T_i	=	ion temperature
t	=	time
t_m	=	round-trip time
t_{m1}	=	minimum t_m with P/m_f constraint
t_{m2}	=	t_m with minimum I_{SP} and $\lvert a\rvert =$ const. constraint
t_{PE}	=	estimated effect of gravity on t_m
V	=	voltage
$\boldsymbol{v}$	=	velocity
v_e	=	orbital speed of the Earth around the sun
v_{Li}	=	velocity of lithium coolant
W/I	=	energy/impulse
Y	=	yield strength
Z_{rt}	=	round-trip distance
β	=	$p/(B^2/2\mu_0)$
ΔT_{max}	=	temperature rise
Δv	=	$\int \lvert a\rvert \, dt$
Δv_f	=	$\int \lvert a\rvert dt$ for the entire trip
δ	=	thickness
δm	=	increment of exhaust mass
ε_{conv}	=	efficiency of converting electricity into exhaust energy
η	=	efficiency, resistivity
θ	=	temperature ratio
λ	=	relaxation global constant $= \mu_0 j/B$
$\lambda(\psi)$	=	$\lambda(\psi)$ is local value of $\mu_0 j/B$
μ_0	=	magnetic permeability of vacuum
ρ	=	mass density
$\sigma \varepsilon r_h T^4$	=	power radiated per unit area of radiator
φ, ψ	=	magnetic flux

I. Introduction

PEOPLE of the future traveling within the solar system might be enabled by fusion direct propulsion devices. Travel times will be short, and the fuel, deuterium, can be found wherever hydrogen exists. Imagine quick trips to interesting solar-system destinations such as Mars, asteroids, Jupiter, Saturn, and even to comets. Human travel throughout the solar system could be possible using spheromak direct propulsion. This paper will outline a spheromak propulsion device for a spacecraft to Europa or Mars, which could also be used for travel to other solar-system destinations. Europa, one of Jupiter's four largest moons, is a very attractive destination. The recent evidence from the Galileo spacecraft shows that under the water-ice shell could lay a vast ocean, warmed by geothermal vents. This potential for an ocean creates a place where life might exist.‡

Human travel to Europa, Mars, and other planets of this solar system by means of chemical propulsion is an overwhelming task. Trip times for chemical propulsion are measured in years, with several gravity-assist maneuvers, and would require large amounts of fuel.

Received 7 July 2004; revision received 13 September 2004; accepted for publication 3 September 2004.

*Professor, Aeronautics and Astronautics Department, P.O. Box 352250. Member AIAA.

†Student, Aeronautics and Astronautics Department, P.O. Box 352250.

‡Data available online at http://www.jpl.nasa.gov/galileo/status970523.html [1997].

The human travelers would be exposed to high amounts of solar radiation as well as microgravity for long durations. The specific impulse of chemical rockets is not suited for routine human travel beyond the moon. The proposed solution is to use a fusion propulsion device to send humans to Europa and back in about a year and to Mars and back in about 100 days.

Although fusion as a terrestrial power source might be decades away, fusion propulsion systems could be developed sooner for the following reasons: First, there is no need to be cost competitive with the existing power grid. Second, the lifetime of the reactor does not need to be as long. Third, because the edge plasma is diverted directly to space to produce thrust, a diverter plate is not required. Fourth, a low-Q, one-pass concept is impractical for power generation on Earth because pumping and fuel reprocessing cost in dealing with the large amount of diverted plasma (which is the rocket exhaust in space) would be prohibitive. Fifth, only the safety of well-monitored small crew is a concern, and a greater risk is tolerable. Sixth, the size of the reactor is not limited to the size that the power-distribution grid will accommodate. Seventh, if launching large amounts of fission fuel is not allowed, there is no other option for practical interplanetary space travel. The deuterium fuel for the spheromak reactor is not radioactive.

There are two types of fusion currently being developed for both power generation and space propulsion applications: inertial and magnetic confinement fusion. Inertial confinement implodes pellets of fuel using a particle or laser beam, thereby creating the reaction. Two examples of studies that have looked into inertial confinement for propulsion applications are DELITE[§] (Earth-orbiting device that propels spacecraft away) and the VISTA, a 60-day trip to Mars concept.[¶] In magnetic confinement, the hot reacting plasma is insulated from the material walls by magnetic field, and the reactor can be steady state. Magnetic confinement has several types of machines capable of creating a fusion propulsion reactor. Examples are tokomaks, stellarators, mirror machines, reversed field configurations, field reversed configurations, and spheromaks. The spheromak was chosen for this study and is the lowest mass concept that has a high-beta, ideal-magnetohydrodymamics (MHD)-stable equilibrium, with close flux surfaces. In addition, it can ohmically heat to ignition, requiring no auxiliary heating system.

A previous study outlined a mission to Saturn using a spherical tokamak fusion reactor.[1] This reactor concept would use ignited D^3He to heat hydrogen and exhaust the hydrogen along with some of the edge plasma from the reactor out a magnetic nozzle to travel to Saturn in 214 days. The spacecraft mass was estimated to be 2640 t, which included a 108-t payload, 45 t of D^3He and 1292 t of hydrogen propellant.

The dimensions of the reactor are as follows: major radius of 2.48 m and minor radius of 1.24 m. The plasma temperature was 50 keV. Other important elements of this reactor are that the reflectivity of the first wall is very high at 98 % and the bootstrap current was overdriven at 1.16 (Ref. 1).

This proposed mission to Saturn would utilize several theories that need more research to prove effective. One of these theories is using helicity ejection with the overdriven bootstrap current to extract electric power from the reactor. Another issue that is not addressed in the research is how the 45 t of ^3He is mined. According to their calculations, to process this amount of ^3He on Earth, with current world production rates of 18 kg/year, would take 2500 years.[1] Even with processing on the moon, where ^3He is more abundant, "processing 40 km^2 of lunar regolith to a depth of 2 m, for example, could yield 1 t of ^3He." Thus, to get 45 t then 1800 km^2 of lunar regolith would need to be processed. Only 1% of the ^3He fuel supplied to the reactor is burned; this study did not look into recycling the ^3He from the exhaust to save on the initial mass of fuel.

The study presented here, using the spheromak fusion concept, requires more progress in plasma science but less progress with other technologies than this spherical tokamak concept. Several other fusion propulsion concepts are discussed in Ref. 2. The spheromak in this paper's study uses only deuterium and exhausts the edge of the reactor plasma directly to space to produce the thrust. The DD fusion reaction is used because no recycling of the fuel from the exhaust is necessary. To formulate what this future spheromak will be like, data from the CTX spheromak experiment are extrapolated to a scaled-up device.[3]

Based on these calculations and assumptions that will be described in this paper, the following mission and reactor characteristics are determined. The round-trip travel time for the mission to Europa is approximately 380 days using 1620 t of fuel to transport the 540 t spacecraft.

In the following sections several questions essential to the design of a spheromak propulsion device are discussed, including why fusion propulsion is necessary for planetary travel as opposed to chemical or nuclear thermal propulsion (Sec. II). Also discussed are the assumptions of how the reactor scales to a propulsion device from current research (Sec. III). Section IV gives the reasons a deuterium-deuterium reaction is chosen over deuterium-tritium and deuterium-helium-3 reactions. The spheromak confinement device, using a bowtie-shaped flux conserver, is discussed in Sec. VI.

Section VI.C discusses how the exhaust is diverted out the spacecraft using conducting ducts to produce thrust. The radiation problems associated with fusion reactors and heat removal using radiators are both addressed in Sec. V. Also given in Sec. V is an introduction to using a gas turbine system for extracting power from the spheromak for the spacecraft. Present research in developing this fusion propulsion power source is discussed in Sec. VI.

By addressing these major questions, an outline for a spheromak propulsion device is created. This propulsion system could serve as the basis for a network of capable spacecraft traveling between the planets. The fast trip times to almost any destination will create a way of transporting supplies and personnel throughout the solar system, allowing human exploration and utilization of our solar neighborhood.

This paper is the first to present a simple, accurate analytic expression for the round-trip times as a function of the power/mass ratio using an optimized, variable I_{SP} that is constained by a lower bound. This paper is the first to explore, in some detail, a DD spheromak as a fusion propulsion concept for interplanetary human travel.

II. Comparison of Chemical, Fission, and Fusion Propulsion Devices

A round-trip mission to Jupiter orbit from Earth orbit requires a specific minimum Δv of about 64 km/s and to Martian orbit requires 14 km/s for a round-trip mission using a minimum propellant, semi-ellipse, impulsive trajectory between Earth's orbit and the target planet's orbit.[4] (Δv is $\int |a|\, dt$, where $|a|$ is the absolute value of the acceleration during the mission.) The round-trip Hohmann transfer time between Earth and Jupiter is 5.48 years, or 2000 days, and 518 days between Earth and Mars.[5] Because a faster trip time is desired, a larger Δv is needed.

A comparison between chemical, nuclear-thermal, nuclear-electric, and fusion types of propulsion systems and the final/initial mass fraction is shown in Table 1. The rocket equation given by

$$m_f/m_0 = \exp(-\Delta v/c_e) \tag{1}$$

is used for chemical and nuclear-thermal systems. The optimum variable c_e as discussed in the next section is used for nuclear-electric and spheromak fusion. The final/initial mass fractions shown in Table 1 are based on round trips to Europa and Mars.

Table 1 shows that the specific impulse for the spheromak reactor and nuclear electric are much more suited for a trip to either destination. For this table, impulse acceleration and deceleration were assumed for the chemical and nuclear thermal cases. Gravity was ignored in all cases because, for the short mission times desired for human travel, it does not make a large contribution to Δv. The initial mass for the fusion case is on a reasonable scale because a new heavy-lift launch vehicle could be capable of lifting up to 250 tons.[1]

[§]Data available online at http://www.islandone.org/APC/Beamed/05.html.

[¶]Data available online at http://www.islandone.org/APC/Nuclear/11.html.

Table 1 Comparison of different types of propulsion

Propulsion type	I_{SP}, s	Round-trip times, days		Final mass/initial mass	
		Europa	Mars	Europa	Mars
Chemical-bipropellant[4]	450	620	175	10^{-9}	10^{-4}
Nuclear-thermal[6]	1000	620	175	10^{-4}	10^{-2}
Nuclear-electric	3,000–20,000	620	160	0.14	0.25
Fusion-spheromak	10,000–40,000	380	100	0.25	0.41

Using this heavy-lift launch vehicle would only require about nine launches to get the spacecraft components including fuel to Earth orbit for the trip to Europa. Obviously the chemical propulsion situation is not practical for high-speed interplanetary travel.

A nuclear-thermal device uses a fission reactor to heat hydrogen propellant to high temperatures. The high-temperature hydrogen is then expanded out a nozzle much the same way the products of a chemical reaction are exhausted. I_{SP} is directly proportional to the square root of the exhaust temperature, which is limited to that of material walls. Thus, a nuclear reactor operates at a much lower temperature than a fusion reactor, and so therefore has a lower I_{SP}. The edge plasma temperatures of the fusion reactor can be varied enough to create very high and variable specific impulses. For the spheromak design the temperature is varied to give close to optimal I_{SP} in order to minimize trip time.

Nuclear-electric propulsion uses a nuclear reactor to produce electricity. This electricity is then used to power an electric propulsion device. There are a wide variety of electric propulsion devices, but the ones most suited for interplanetary travel are ion engines and Hall thrusters. For the table, the optimum I_{SP} above 3000 s is used. A power-to-mass ratio, based on Sec. V.E, of 0.375 kW/kg is used. The power to mass ratio is P/m_f. We have the technology to build such a power system today.

With the fusion spheromak propulsion, for the table, the optimum I_{SP} above 10,000 s is used. A power-to-mass ratio, based on Sec. V.E., of 1.84 kW/kg is used.

III. Mission Times vs Power-to-Mass Ratio

For fusion propulsion (and also nuclear-electric) the key parameter that limits mission times is the power-to-mass ratio that can be achieved. The big advantage to these methods, at least for interplanetary travel, is that they can produce an optimum, variable I_{SP}. For nuclear-electric the I_{SP} is controlled by the operation of the plasma thruster. In direct diverted fusion propulsion the I_{SP} is controlled through the edge temperature, which is controlled by the rate and depth of fueling. Fueling control is an important part of developing magnetically confined controlled fusion.

There are two energy costs associated with making rocket exhaust. One is that spent at the time the exhaust is expelled, and the other is the kinetic energy the fuel has from being onboard the rocket. Define the relative kinetic energy as $\frac{1}{2}m\Delta v^2$, where m is the mass of the rocket and fuel. The best that can be achieved is for all of the energy that is spent expelling exhaust to be in the relative kinetic energy of the rocket and remaining fuel. In a gravity-free space this is achieved when the exhaust speed is varied to always equal Δv. (It is assumed, for this section, that all of the exhaust is produced with the optimum speed at 100% efficiency.) In a simple acceleration this condition leaves the exhaust at rest in the initial frame. Thus, the exhaust has zero kinetic energy, and the rocket has all of it. The relative momentum $m\Delta v$ is constant. In this case, as shown in Appendix A, if the power is constant, the acceleration is constant. By using relative energy and momentum, this result also applies to rendezvous and return missions as well, which are the topics of this section.

Define m_f and Δv_f as the final mass and Δv where all of the fuel is spent and the mission is complete. Let P be the power that is put into exhaust by the propulsion unit part of this m_f. The absolute value of acceleration and deceleration $|a|$ for the entire mission is just $2P/m_f\Delta v_f$ (see Fig. 1 for the velocity and Δv of a rendezvous and return mission).

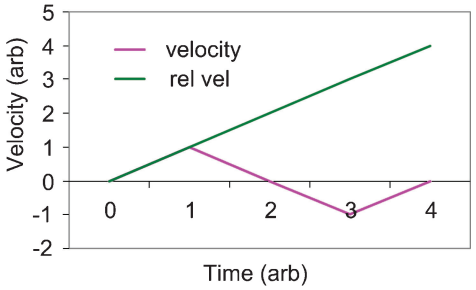

Fig. 1 Velocity and relative velocity vs time for a rendezvous and return mission with constant acceleration.

The mission has four equal length segments of length $\frac{1}{2}a(t_m/4)^2$ each. Thus, with simple algebra the round-trip time for gravity-free space and only a P/m_f constraint is given by

$$t_{m1} = 4\left(\frac{m_f Z_{rt}^2}{2P}\right)^{\frac{1}{3}} \tag{2}$$

In practice, there is a lower limit on the exhaust velocity and an upper limit on the amount of initial fuel mass for the mission. To realize Eq. (2), an infinite initial mass is required because the relative momentum is constant and the initial velocity is zero. Nonetheless, this equation gives the shortest possible mission time for comparison purposes. For fusion propulsion with single pass deuterium, the exhaust speed must be high enough so that the ionization cost (about 50 eV per D) is considerably less than the kinetic energy of the exhausted D atoms. Choosing 100 eV for the initial exhaust energy puts a lower bound on the initial exhaust speed c_{ex} of 100 km/s. As will be shown, this also gives a practical initial fuel mass for interplanetary missions. As long as c_{ex} is small compared to Δv_f, the mission times can approach that of Eq. (2). Therefore, a constant acceleration is chosen for this problem as well, and the exhaust speed is chosen to be $c_e = c_{ex} + \Delta v$. The mission time is then given by the following:

$$t_{m2} = 4[(m_f Z_{rt}/P)(Z_{rt}/2 + c_{ex}t_{m2}/16)]^{\frac{1}{3}} \tag{3}$$

Although this is a cubic equation for t_{m2} (the mission time) that has an exact solution, an iterative solution converges very rapidly for the most interesting cases when $Z_{rt} \gg c_{ex}t_{m2}/8$ is satisfied. Equations (2–4) are derived in more detail in Appendix A.

In Eqs. (2) and (3) the effect of gravity was ignored. The biggest gravitational potential change is caused by changing of the solar orbit. The amount this changes the trip time should be less than that needed to accelerate the rocket from rest to the velocity needed to reach the mission orbit from Earth orbit. This time t_{PE} is given by

$$t_{PE} = v_e\left(\frac{Z_{rt}}{Z_{rt} + 2R_e} \cdot \frac{m_f t_m}{2P}\right)^{\frac{1}{2}} \tag{4}$$

The actual increase in an optimized mission time can be considerably less than this because the sun's gravity helps on about half the trip and hurts on half the trip to give offsetting total effect. The magnitude of the effect is given by t_{PE}. Figure 2 shows the three times t_{m1}, t_{m2}, and t_{PE} as a function of P/m_f for a mission to Mars. Figure 3 shows the three times as a function of P/m_f for a mission to Jupiter orbit.

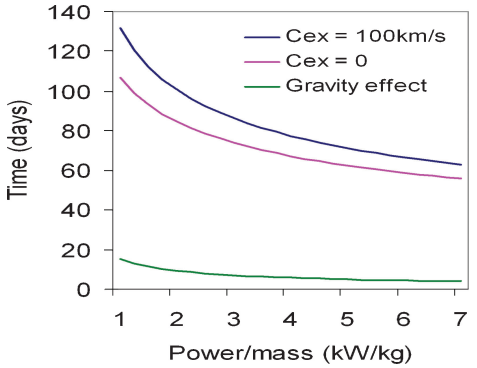

Fig. 2 Round-trip travel time to Mars with constant acceleration. The upper curve is for a minimum exhaust speed of 100 km/s. The middle curve is with no minimum and represents the minimum possible time but requires an infinite initial mass. The bottom curve shows how gravity could increase the time.

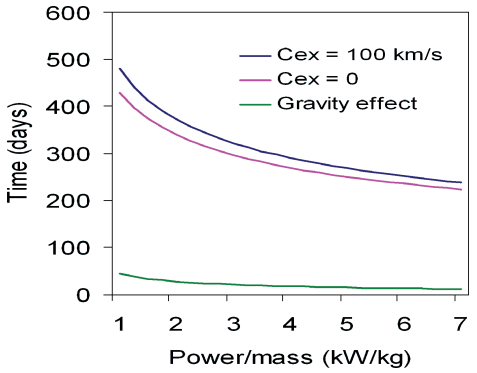

Fig. 3 Round-trip travel time to Europa with constant acceleration. The upper curve is for a minimum exhaust speed of 100 km/s. The middle curve is with no minimum and represents the minimum possible time but requires an infinite initial mass. The bottom curve shows how gravity could increase the time.

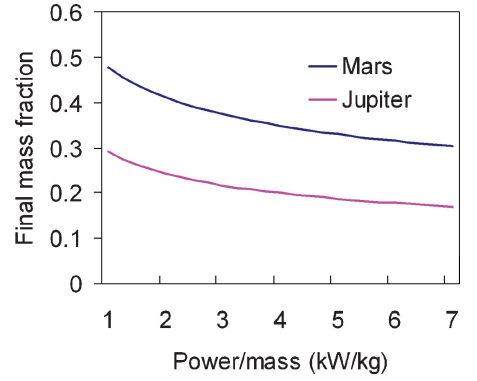

Fig. 4 Final/initial mass fraction for the Mars and Europa missions with constant acceleration and an initial minimum exhaust velocity of 100 km/s.

Figure 4 shows the final/initial mass fraction at the beginning of each mission [from (low Earth orbit)] as a function of P/m_f for the case where $c_{ex} = 100$ km/s.

Increasing P/m_f shortens the mission time. However, the weak cube root dependence means that large improvements in P/m_f must be made to significantly shorten the time. A spheromak reactor study that was not optimized for low mass[7] found a P/m_f of 1.2 kW/kg. The present study shows that 1.84 kW/kg can be possible soon after fusion power is generated with the spheromak concept.

Raising the initial exhaust speed c_{ex} increases the mission time but reduces the initial fuel requirements. As long as $c_{ex}t_m/8$ is small compared to Z_{rt}, there is little increase in mission time from raising c_{ex}, and a large decrease in initial fuel mass might be possible. For example, raising c_{ex} from 100 to 141 km/s increases the Europa mission time (at $P/m_f = 3$ kW/kg) by 2% while increasing the final/initial mass fraction by 30%.

In fusion propulsion using single pass deuterium, a c_{ex} of 100 km/s is probably about as low as would be desirable because the relative ionization costs would become large at lower speeds. This value gives very reasonable final mass fractions while still yielding mission times within 10% of the shortest possible time for a given power-to-mass ratio for Europa and 20% for Mars. These estimates ignored the effects of gravity, which are also shown to be an even smaller effect. The most conservative upper bound on the round-trip time would be to add t_{m2} and t_{PE}. Thus, the results of this section bracket the minimum round-trip time with finite c_{ex}. A true optimization for the minimum mission time as a function of power-to-mass ratio and the lower bound on the exhaust speed, including gravity, would be very interesting.

When applied to much higher P/m_f, the results from this analysis are in rough agreement, both in the absolute times and scaling with those of Williams.[8] For example, at $P/m_f = 100$ kW/kg and $c_{ex} = 0$, 92 days are required for the round-trip Jupiter mission, which is about 20% shorter than reported in that reference. Also, $P/m_f = 100$ kW/kg and $c_{ex} = 380$ km/s gives a 25% initial pay load fraction and 102 days for the round-trip Jupiter mission, which is about 30% shorter then reported in that reference. As stated in that reference, gravity effects are insignificant for this very large P/m_f regime.

IV. Using DD Fusion

Both tritium (T) and helium 3 (^{3}He) are very rare. Tritium has a 12-year half-life and does not exist in any significant quantity in nature and must be bred by the fusion reactor. The DT reaction produces one neutron, which is used with lithium (Li) to generate one T. The neutron can be multiplied by interacting with wall material or with ^{7}Li. Breeding ratios of over one are possible, but large factors like two are not. Thus, the reactor cannot afford to lose T. At least $\frac{2}{3}$ of the T produced must be burned. Because the energy deposited in the plasma by one fusion reaction is over 2000 times the energy of one exhausted particle, over 2000 particles must be exhausted to use up this energy. If the plasma is about half T, there are about 1000 T exhausted for each T produced. Affordable losses can only be about one-fifth the amount produced. Thus a T recovery method can only lose one in every 5000 recovered T. Otherwise, T will be lost faster than it is produced. In addition, about $\frac{3}{5}$ of the mass outflow is lost in not letting the T escape. Thus, a D-T fusion reactor is not feasible or practical for this propulsion device. D^{3}He has the same problem because ^{3}He is so rare that it is not feasible to have a significant fuel mass in ^{3}He. Therefore, probably the only way DT or D^{3}He fusion would be practical is to run the fusion reactor with a closed gas cycle and just generate electricity for electric propulsion similar to nuclear-electric methods.

Another solution is to make a DT or D^{3}He reactor with such good confinement that 80% of the fuel is burnt in a single pass through the reactor. However, such confinement, when the ^{4}He ash effects are taken into account, is high enough to burn pure deuterium, which is abundant enough that un-burnt D can be used for inert fuel mass. With two-thirds burned up, the exhaust would be $\frac{1}{4}$ D, $\frac{1}{4}$ T, and $\frac{2}{4}$ ^{4}He. Assuming the same mix throughout the volume, the reaction rate would be $\frac{1}{4}$ of that without the ^{4}He. The reaction rate is proportional to the product of the density of D times that of T. With no ^{4}He they would each be half the total density instead of $\frac{1}{4}$. Except for the burn-up constraint only about 7% burn up is required. An additional factor of 10 in confinement is needed to achieve the 67% burn up. Thus, the high burn-up requirement increases the total confinement needed by about a factor of 40. However, the reaction rate of DD is a factor of 40 less than DT at a temperature of 50 keV. Thus, the best solution is a single pass DD reactor having an engineering Q just above one when considering only the neutron power, with the edge plasma diverted to make the rocket exhaust. Having the inert fuel being the same as the thermonuclear fuel also facilitates heating the inert fuel without contaminating the reacting plasma.

V. Spheromak Fusion Reactor

A. Scaling to a Fusion Propulsion Unit and Other Assumptions

The spheromak reactor physics used in this study is based on scaling from the experimental results from the Los Alamos CTX spheromak experiment.[3] The spheromak was formed with electrostatic helicity injection using a coaxial magnetized Marshall Gun and then allowed to decay. During the decay, the spheromak was ohmically heated to its β limit.[9] The temperature ($\approx$0.4 keV) and confinement were limited by the consequences of reaching this limit. In these experiments, the shapes of the boundary and the current profile were not optimized for high β. Most of the high-temperature plasma was at a higher β in a fraction of the entire volume. Therefore, for the scaling we assume 1) the spheromak sustained with helicity injection current drive has sufficient confinement to ohmically heat to the β limit. This is justified because decaying spheromaks are observed to ohmically heat to the β limit and the scaling of the fluctuations levels required to sustain a hotter plasma should decrease to improve the confinement by more than the loss of heating. However, this is a very important question that is being studied in spheromak controlled fusion research, and a favorable outcome is assumed.

Also assumed is that 2) the resistivity scales approximately like Spitzter resistivity ($\propto T^{-3/2}$) and 3) the efficiency of the sustainment of the magnetic energy is 50% for the power delivered to the spheromak and 90% efficiency in power conditioning from the generator to the spheromak. Assumption 2) is justified because a relaxed stable plasma will be left with only collisional resistivity that scales like Spitzer. In assumption 3) we allow for the "anomalous" resistivity caused by helicity conserving relaxation. Experience to date indicates that 50% loss of injected power caused by relaxation is typical. Although it might be possible to improve this, we stick with proven results. With modern power handling methods 90% of the electricity from the generator can be delivered to the spheromak.

The volume-averaged betas of over 10% are calculated for the bowtie geometry and were observed in the "tuna can" geometry of the Los Alamos experiments.[3] Most of the plasma is near the magnetic axis at much higher than 10% beta. Of course, beta is zero at the edge. To estimate reactivity and radiation losses, β, calculated using the volume-averaged B^2, is assumed 4) to be 30% over one-third the volume and zero elsewhere, giving the 10% volume-averaged β. The spheromak edge fields are lower than the volume average so that the engineering beta ($2\mu_0 p/B_{\text{ext}}^2$) is 43% over one-third the volume. This is a simplifying assumption, but it would be unrealistic and pessimistic to assume a uniform 10% beta for this 0D model. For example, in a tuna can experiment that reached the β limit, the peak of the electron pressure before instability was 20% of the volume-average magnetic pressure.[9] Assuming $T_e = T_i$, the β was 40%, based on volume-averaged magnetic field. Taking into account the decrease in the local field caused by that pressure, the local β was over 60%. The half-maximum minor radius of the pressure was 0.12 m, and the minor radius of the plasma was 0.3 m for a plasma volume of 16% of the total. Considering these results, this assumption is very conservative.

Based on the spheromak reactor study,[7] the neutron wall loading is assumed 5) to be limited to 20 MWm^{-3}. (Actually, 13.5 MW/m^2 is used.) The burn-up fraction of all of the deuterium and reaction products is based on the confinement time required for ohmically heating the plasma to the 50 KeV. It is assumed 6) that the particle confinement times in the burning plasma regions is equal to the energy confinement time. This yields 15%, 42%, and 100% burn-up fractions of D, ^{3}He, and T, respectively. The ^{3}He reaction provides about half of the fusion power to the plasma. Most of the exhaust plasma is produced by passing deuterium through the edge at the correct rate so that it is heated to the temperature required for the desired I_{SP}.

The tank masses and radiation shielding mass required to contain and shield the D fuel is assumed 7) to be small. With the weightlessness of space and the very small acceleration of the rocket, the force to contain the fuel is very small so that the tanks can be extremely low mass. Thus, fuel tank mass is very small compared to the fuel mass, a few percent at most. In the vacuum of space, only radiation shielding is required for insulation, which would be layers of very thin metal foil. Shadowing the sun and the power radiators would be the main task. The tanks would be jettisoned when they are empty, and their mass does not add to m_f. Their impact on the mission times will be small. The power/mass ratio is effectively lowered by a fraction equal to half of the tank/fuel mass ratio. (Jettisoning the empty tanks wastes their kinetic energy, but that is only half the energy given to normal fuel.) This effect is much smaller than the uncertainties in our estimates given in this paper.

Table 2 Parameters scaled up from CTX experiment

Parameter	CTX(1990)	Reactor	R^n scaling
Vessel radius and length, m	0.28	3.13	$n=1$
Toroidal current, MA	0.78	98	2
Magnetic field at wall, T	1.0	11	1
Magnetic energy, MJ	0.054	9579	5
Temperature, keV	0.4	50	2
Magnetic decay time, s	0.001	175	5
Sustainment power, MW	110	110	0
Fusion power to plasma, MW	n/a	954	n/a
Fusion power in neutrons, MW	n/a	1360	n/a

The reflectivity of the first wall to synchrotron radiation is conservatively assumed 8) to be 90%. There are wall materials that have higher reflectivity such as optical beryllium,[1] but the continuous use of the reactor and plasma interaction with the wall causes the wall to become less reflective, therefore increasing the power losses to radiation. Also because the edge plasma is diverted to form the propulsive exhaust, the portions of the wall where the plasma escapes are not reflective. Especially at the synchrotron radiation wavelengths, a reflectivity of at least 90% is attainable. This is conservative compared to the 98% assumed in Ref. 1.

Table 2 shows some of the key parameters of the experiment and the proposed fusion propulsion reactor. In addition to the preceding assumptions, the scaling assumes constant: current density ($j = 10$ MA/m^2), volume-averaged density ($n = 4.2 \times 10^{20}$ m^{-3}), and β. This gives a j/n of 2.4×10^{-14} Am, which is an acceptable value. The extrapolation is large, but current research is underway to test and develop this concept as discussed later. The size is chosen for 50 keV, which is optimal for a DD reactor.

B. Radiation Concerns

There are several types of radiation emitted from the spheromak reactor. Two types that present a significant source of power loss to the reactor are synchrotron radiation P_{syn} and Bremsstrahlung radiation P_{brem}. The equations for the power loss from both types of radiation are given next.[10]

In Ref. 10 synchrotron radiation is discussed in terms of the length of a slab L of plasma needed to provide the power radiated from the DD reaction alone. It gives

$$L \propto \left[g^2(T) \Big/ \beta_e^3 B \right] \tag{5}$$

and quotes a value $L = 0.32$ m with $\beta = 0.4$, $B = 10$ T, $T = 50$ keV, and reflectivity $= 0.9$. In the plasma proposed here, β and B are 0.43 and 9 T, respectively, giving $L = 0.28$ m. The power loss by synchrotron radiation is then the DD particle power to the plasma reduced by L/(plasma minor radius).

Bremsstrahlung radiation is given by

$$P_{\text{brem}} = 5 \times 10^{-37} n^2 T_e^{\frac{1}{2}} \ (\text{W/m}^3) \tag{6}$$

where the number density n is in m^{-3} and T_e is in keV. Using these equations for a 3.13-m DD burning, spheromak reactor, the power losses caused by radiation are 124 MW of synchrotron radiation and 180 MW of bremsstrahlung radiation. (The plasma minor radius is 0.9 m.)

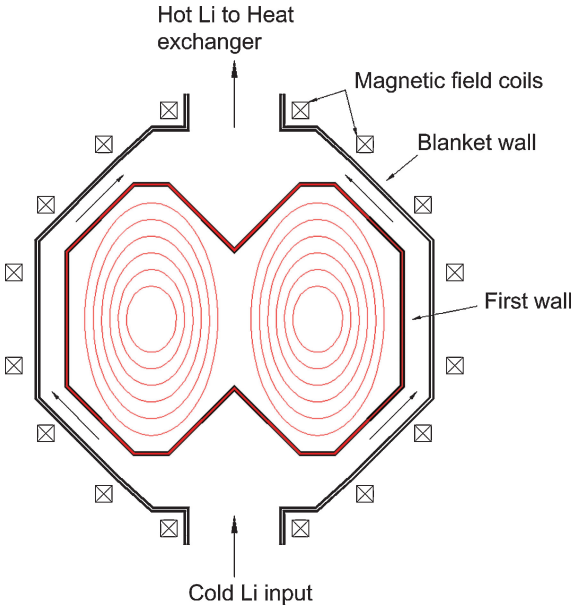

Fig. 5 Diagram of spheromak with first wall, blanket, and equilibrium coils.

C. Reactor Structure and Blanket

The spheromak reactor structure has coils to create the magnetic fields, a first wall able to take the extreme heats and pressures, and a cooling blanket as well as heat exchangers. Figure 5 shows a diagram of all of these elements.

The equilibrium coils create the magnetic confinement of the fusion plasma. Superconducting material is used for the coils based on a lower mass than other options. The material for the coils is Nb_3Sn wires. The wires are stabilized by copper filaments, and liquid helium is used as a coolant in the coils. This configuration has demonstrated current densities of as high as 3×10^9 Am^{-2} with magnetic fields up to 12 T (Ref. 11).

For a plasma current of 98 MA, a total superconducting cross section of $\sim$0.033 m^2 is therefore needed. An average coil radius of 3.4 m, and a mass density of Nb_3Sn of approximately 9000 kg/m^3 translates to a superconductor mass of about 7 metric tons. Nb_3Sn wires are typically manufactured with copper/noncopper ratios greater than 1, meaning that the total mass of the coils would actually exceed 14 tons. Because of the necessity to maintain the superconductor below liquid helium temperature (4.2°K), a coil-to-coolant-infrastructure mass ratio of 1:2.5 was assumed, adding 38 tons to the mass estimate, while power requirements for the refrigeration system are assumed to be negligible (<1 MW) (Ref. 1).

The coils, however, are also subject to a large $B^2/2\mu_0$ magnetic pressure so that they must be held using a material with a high strength-to-mass ratio. Titanium alloys, specifically Ti-6A1-4V, have a high yield strength of $Y = 1.9 \times 10^9$ N/m^2. The mass of Ti needed to support the coil is estimated by calculating the thickness needed for a uniform pipe to hold the magnetic pressure. For a safety factor of S, the thickness needed is given by

$$\text{thickness} = \left(SB^2 r \big/ 2\mu_0 Y\right) \tag{7}$$

where r is the radius, set at 3.4 m, the magnetic field is given as B and is 11 T, then the thickness is about 0.19 m, assuming a safety factor of 2. Using a density of the titanium of 4400 kg/m^3 and a length of 3.13 m, this supporting structure adds 60 t to the coil structure. In Fig. 6 the coil cross section is shown with titanium support structure, superconducting filament, copper structure, and cooling channels.

The conducting liquid lithium coolant in the blanket region acts as a flux conserver for high-frequency wall-stabilized plasma modes. The skin time of the 0.275-M-thick hot lithium, with a resistivity of 3.0×10^{-7} Ω-m, is about $\frac{1}{6}$ of a second and will stabilize modes with frequency above about 1 Hz. Thus, low-frequency feedback stabilization will be necessary to stabilize lower-frequency modes like the resistive wall modes. Pumping the liquid parallel to the large edge magnetic field ($\sim$11 T) minimizes any ohmic losses and additional heating of the lithium caused by $\boldsymbol{v} \times \boldsymbol{B}$ induced currents.

Table 3 Summary of the lithium blanket characteristics

Characteristic	Value
Lithium thickness	0.275 m
Resistivity (lithium)	3×10^{-7} Ω-m
Flow velocity	0.1 m/s
Blanket mass	25–30 mt
High temperature	1400 K
Low temperature	600 K

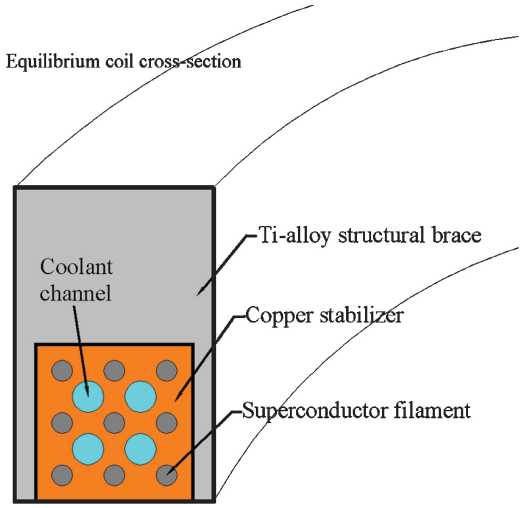

Fig. 6 Equilibrium coil cross section.

The lithium blanket also serves to remove heat and absorb the high-energy neutrons from the DD reaction. The T produced in the blanket can be stored and used for reactor startup and also can be used as fuel at the end of missions where a higher burn-up fraction is needed for the higher I_{SP}. The reactor emits neutron and radiation for a wall loading of 13.5 MW/m^2. The lithium flow rate is found by assuming that the heating is uniform, and a temperature rise $\Delta T_{\max}$ is desired for power generation. The relation

$$Qt \leq C_v \delta \Delta T_{\max} \tag{8}$$

is used where Q is the heat flux, t is the transit time of the coolant, δ is the thickness, and C_v is the volumetric heat capacity. Assuming a uniform heat transfer and conduction in the blanket over one traversal of the entire reactor length L_{rctr}, the velocity requirement is found by solving Eq. (8) for t and substituting into $v_{\text{Li}} = L_{\text{rctr}}/t$:

$$v_{\text{Li}} \geq \frac{QL_{\text{rctr}}}{C_v \Delta T \delta} \tag{9}$$

Using a blanket thickness of 0.275 m, a reactor length of 3.13 m, $Q = 13.5$ MW/m^2, $C_v \approx 1.8 \times 10^6$ $J/(m^3 \cdot K)$, and $\Delta T = 800$°K, the velocity of the lithium pumped through the reactor blanket is approximately $v_{\text{Li}} \geq 0.1$ m/s. A summary of the blanket characteristics is shown in Table 3. Approximately 10 metric tons of lithium is required to fill the blanket volume once. Additional material is necessary to complete the heat-exchanging circuit and fill the pumping reservoir volume. More mass is needed to provide structural support capable of retaining strength at the high blanket temperatures. A rough estimate of between 35–40 metric tons for the total blanket mass is used.

Table 4 summarizes the mass estimates for the blanket and coil structures of the reactor.

D. Electricity Generation

A closed helium gas turbine cycle is proposed to be suitable for the power conversion system of a fusion-powered spacecraft. Helium is chosen for its high heat capacity, inert nature, and its low density. For source temperatures more than 800 K, a highly recuperated Brayton cycle is the most efficient cycle available.[12] The power conversion efficiency of a simple Brayton cycle with a regenerator (recuperator) is estimated. Figures 7 and 8 illustrate the schematic of the simple Brayton cycle and the corresponding temperature (T)-entropy (S) diagram.

An ideal Brayton cycle is composed of two isentropic processes and two isobaric processes, which make the efficiency of the cycle only depend on the temperature ratio, or the pressure ratio.[13]

$$\eta_{\text{ideal}} = 1 - (1/r_p)^{(\gamma-1)/\gamma} \tag{10}$$

Here γ is the common, specific heat ratio. The existence of irreversibility of the turbine and the compressor (the dashed lines in Fig. 8) causes a decrease of the cycle efficiency. The adiabatic efficiencies of the working components and the efficiency of the recuperator are chosen based on Ref. 12.

The principal design parameters used in the calculation are the following: adiabatic efficiency of the turbine $\eta_t = 0.93$; adiabatic efficiency of the compressor $\eta_c = 0.90$; efficiency of the recuperator $\eta_{Re} = 0.95$; pressure ratio $r_p = P_2/P_0 = P_4/P_5$; temperature ratio $\theta = T_4/T_0$; and mass flow rate of the working gas (helium) $\dot{m}$. With a given power input and the temperature at the high-temperature reservoir ($T_4 = 1400$ K), the temperature ratio and the mass flow rate determine the cycle efficiency. A high-temperature ratio requires a large radiator mass to radiate power to space at a low temperature. A high mass flow rate requires more rotating machinery mass. For a given efficiency there is an optimum combination for the minimum total mass. The radiator mass strongly depends on the temperature of the working fluid at the inlet and the outlet of the radiator. The mass value of the carbon duct (1.25 kg/m^2) is given in Ref 1. The radiator mass can be estimated using

$$A = \int_{T_0}^{T_6} \frac{C_p \cdot \dot{m}}{\sigma \cdot \varepsilon \cdot r_h} \cdot \frac{1}{T^4} \cdot \mathrm{d}T \tag{11}$$

Table 4 Summary of reactor blanket and coil masses

Component	Mass, t
Bulk Li coolant	25
Blanket structure	~ 12
Total blanket mass	~ 37
Superconductor + copper stabilizer	14
Mechanical support structure	60
Cryogenic systems	38
Total equilibrium coil mass	~ 112
Total blanket and coil mass	**~ 150**

where $\sigma \varepsilon r_h T^4$ is the power radiated per unit area, C_p is the heat capacity, and A is the radiator area. The mass of recuperator, turbine, ducts, and supporting structure is assumed to be proportional to the mass flow rate of the working fluid (helium) with the ratio of 90 s, taken from Ref. 1. At each efficiency, this subsystem, including the radiators, is optimized for the maximum shaft power per kilogram. This shaft power is delivered to the alternator. In the second subsystem, the mass of the alternator, power conditioning and distribution equipment, low-temperature radiators for cooling electrical equipment, and support structure is assumed to be proportional to the power generated. The ratio for this subsystem is assumed to be 5 kW/kg, again consistent with Ref. 1. These solutions for the two subsystems are then combined for the maximum $P_{\text{elc}}/m_{\text{elc}}$ at each efficiency, where P_{elc} is the electrical power out and m_{elc} is the total mass of the two subsystems. The result is shown in Fig. 9.

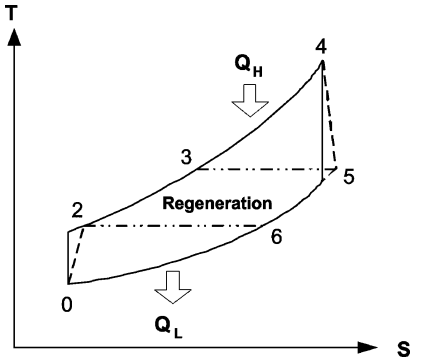

Fig. 8 Temperature-entropy plot for an ideal Brayton cycle.

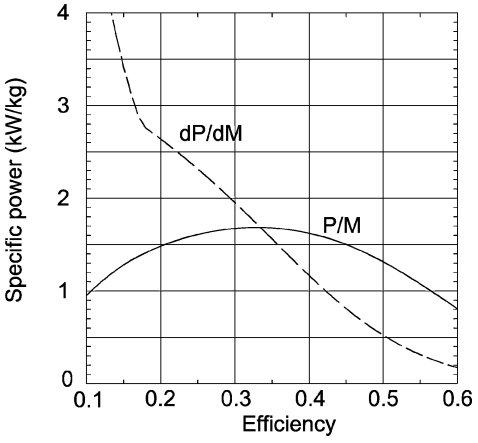

Fig. 9 Optimum $P_{\text{elc}}/m_{\text{elc}}$ (solid curve) and $\mathrm{d}P_{\text{elc}}/\mathrm{d}m_{\text{elc}}$ (dashed curve) as a function of efficiency at $T_4 = 1400$ K. T_0 varies nearly linearly from about 800 K at $\varepsilon = 0.1$ to 400 K at $\varepsilon = 0.5$.

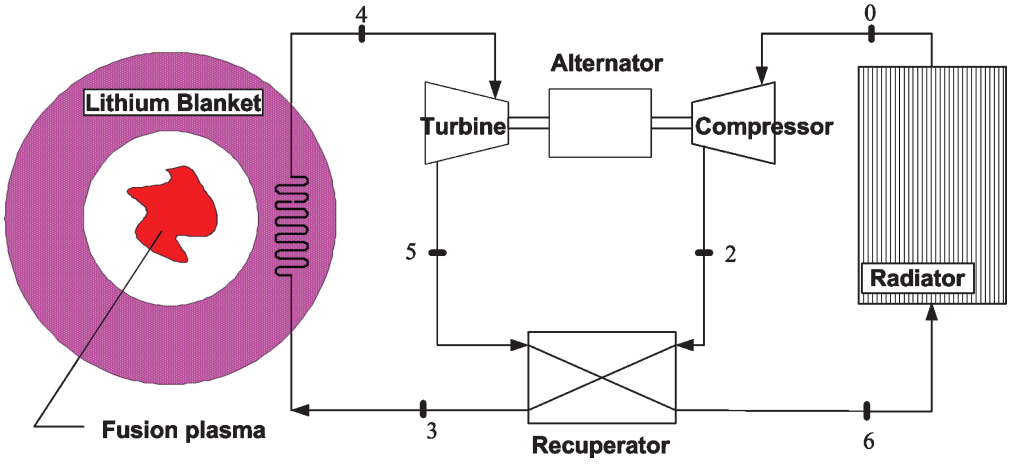

Fig. 7 Schematic of gas turbine power cycle.

Also calculated is the corresponding dP_{elc}/dm_{elc} while following the P_{elc}/m_{elc} curve. The dP_{elc}/dm_{elc} at fixed input power is needed for optimization. If $\varepsilon_{conv} dP_{elc}/dm_{elc}$ is greater than P/m_f (defined in Sec. III), the efficiency should be increased, where ε_{conv} is the efficiency of converting electricity into exhaust energy (assumed 0.9). If it is less, the efficiency should be decreased. The optimized electrical generation system should operate at $P/m_f = \varepsilon_{conv} dP_{elc}/dm_{elc}$.

In this particular example, P/m_f is about 1.84 kW/kg and $\varepsilon_{conv} dP_{elc}/dm_{elc}$ is equal to this at an efficiency of about 0.29. Therefore, the best P/m_f is achieved at this efficiency for electrical conversion.

The turbine and generator can also be used as an energy storage device to provide the necessary energy for reactor startup. Although this stored energy would be less than the magnetic energy for DD operation, it would be enough for a DT startup that could then transition to DD operation. The initial spin-up of the turbine and generator could come from chemical energy.

E. Overall Power Flow and Total Mass

The spheromak reactor produces 2658 MW of power. This power is mainly directed into space either as thrust or as radiation to the walls. However, the reactor and spacecraft are sustained by a fraction of this generated power. The flowchart in Fig. 10 shows the power distribution of the spacecraft. Although 110 MW are required to sustain the plasma current, the optimum amount of 344 MW is given to the spheromak. The extra capacity is also valuable for startup and as a safety factor. The reactor Q (power out/power in) is only seven. It is assumed that the input power and the power from fusion-produced charged particles is converted into P_{brem}, P_{syn}, and exhaust power for thrust by the plasma. The total mass is 540 metric tons.

Table 5 shows the major components of the mass. The 100 t for "life support and others" is based on the results of Ref. 1.

Thus, the power-to-mass ratio is 1.84 kW/kg requiring about 100 days for travel to and from Mars and about one year to and from Europa. (There is not a weight growth contingency in these estimates. Adding 30% more mass for contingency would increase the times by about 10%.) These should be acceptable mission times because they are similar to the time to circumnavigate the globe in the 19th (Nellie Bly) and 16th (Ferdinand Magellan) centuries, respectively.

A 575-t pressurized-water fission reactor can generate 1600 MW of heat.[7] From Fig. 9 this heat can be converted to about 720 MW of exhaust power with 600 t of generator and radiators with a power

Table 5 Spacecraft's component mass and total mass m_f

Component	Mass, t
Reactor	150
Electricity generation and radiators	290
Life support and others	100
Total	540

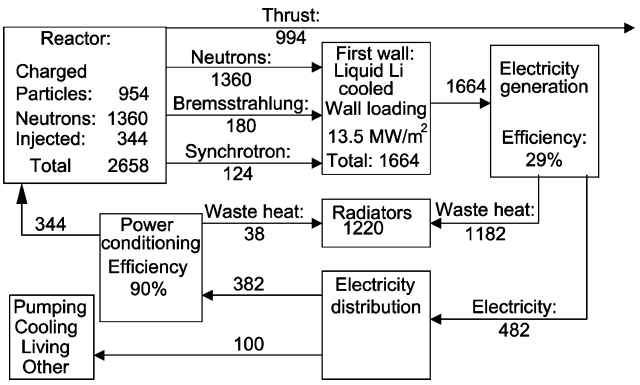

Fig. 10 Flowchart of the power distribution in the spacecraft in megawatts.

generation efficiency of 0.5 and power conditioning efficiency of 0.9. It might take about 650 t of ion thrusters to convert the 720 MW of conditioned power to exhaust.[4] Adding 100 t for living and other needs, the total mass is 1925 t for a power-to-mass ratio of about 0.375 kW/kg, which was used for Table 1. A more careful system study and optimization might allow nuclear-electric to achieve even larger power to mass ratios.

VI. Reactor Concept

The experiment that was scaled for the basic reactor parameters just used had electrostatic helicity injection, which is discussed next, with the edge open field lines landing on electrodes and not diverted into space.[3] The shape was a simple tuna can shape, which does not lead to high beta in a reactor.[3,14,15] The higher beta bowtie shape is not very compatible with helicity injection using coaxial electrodes. These considerations plus the fact that magnetic confinement has had greater success with inductive driven machines leads to the conclusion that inductive helicity injection might be superior. With inductive helicity injection, the very edge, open field line and plasma can be diverted into space for thrust and the adjacent closed field plasma driven with the inductive injectors.

A. Helicity Injection Current Drive in General

Reversed field pinch and spheromak experiments and considerable theoretical analysis have shown that magnetic helicity (defined next) is the best constant of the motion of a magnetized plasma.[15–17] The Taylor minimum energy principle states that, in a plasma, magnetic fields relax to a state of minimum energy while conserving magnetic helicity. If relaxation is complete, then $\nabla \times \boldsymbol{B} = \lambda \boldsymbol{B}$, where λ is a global constant.[18] Utilizing Ampere's law yields $\lambda = \mu_0 j/B$. This understanding is valuable in predicting the effects of instability on magnetic profile evolution. Namely, if the plasma boundary is a helicity barrier, magnetic activity will conserve helicity and flatten the $\mu_0 j/B$ profile. Therefore, driving j high in one region of the plasma leads to current drive throughout the plasma volume. Helicity injection current drive is simply driving current high in the region of the plasma that is most convenient and allowing relaxation to produce the current throughout the volume.

Helicity conservation plays a key role in dictating that magnetic activity, which impedes current in the high $\lambda(\psi)$ regions, must also drive current in the low $\lambda(\psi)$ regions, where $\lambda(\psi)$ is the local value of $\mu_0 j/B$. Because any region of low $\lambda(\psi)$ inside the helicity barrier can absorb and dissipate helicity, open field lines in the edge regions such as behind a limiter must be avoided as undesirable helicity sinks. Indeed, such regions on reverse field pinches (RFPs) and spheromaks increase the anomalous resistivity and severely degrade confinement.[19,20] Thus, open field lines degrade performance and should be avoided. Because the current increases when the helicity increases and helicity is the most conserved quantity, it is the most important quantity to inject.

Helicity is the linkage of magnetic flux with magnetic flux, and the helicity from the linkage of flux tubes φ_1 and φ_2 is $2\varphi_1\varphi_2$ (Ref. 21). As flux becomes linked or unlinked, an electric field is produced parallel to the magnetic field. If the magnetic field penetrates or links the boundary, then the linkage is uniquely defined such that the vacuum helicity is subtracted giving the simple relation for the change of helicity as

$$\frac{dK}{dt} = 2\int \boldsymbol{E}_v \cdot \boldsymbol{B}_v \, dvol - 2\int \boldsymbol{E} \cdot \boldsymbol{B} \, dvol$$

where K is the helicity, $\boldsymbol{E}$ and $\boldsymbol{B}$ are the electric and magnetic fields in the plasma, and $\boldsymbol{E}_v$ and $\boldsymbol{B}_v$ are the electric and magnetic fields for the vacuum case with the same $\boldsymbol{E}$ parallel and $\boldsymbol{B}$ normal to the boundary and the same flux linking the boundary as in the plasma case. The integrals are done inside the plasma volume.[15] The first term on the right is the helicity injection term, and the second is the dissipation. Helicity injection can be electrostatic or electromagnetic.[22] Usually, helicity is injected by applying a voltage V_{inj} to some flux ψ_{inj} that either penetrates electrodes (for electrostatic injection) or links the boundary (for electromagnetic injection). The injection term is then

$2V_{\text{inj}}\psi_{\text{inj}}$, where V_{inj} is the voltage between the electrodes in the electrostatic case or the loop voltage in the electromagnetic case. For example, in a transformer driven tokamak or RFP, the helicity injection rate is $2V_{\text{loop}}\Phi_{\text{tor}}$. From the minimum energy principle, helicity is dissipated only by resistive diffusion. Therefore

$$\int \boldsymbol{E}\cdot\boldsymbol{B}\,\mathrm{d}vol = \int \eta\boldsymbol{j}\cdot\boldsymbol{B}\,\mathrm{d}vol$$

However, $\boldsymbol{E}$ does not equal $\eta\boldsymbol{j}$ at each point because relaxation activity produces anticurrent drive in regions of high $\lambda(\psi_H)$ and current drive in regions of low $\lambda(\psi_L)$.

B. Steady Inductive Helicity Injection Current Drive

Steady inductive helicity injection has constant inductive helicity injection on the bowtie spheromak. For inductive drive, the time-averaged voltage on one injector is zero with the voltage passing through zero. Thus, for constant injection two injectors must be used so one can inject during the zero crossing of the other. To prevent helicity ejection when the voltage is negative, the flux must change sign with the voltage. The HIT-SI experiment is among the simplest that can meet these requirements and be compatible with the bowtie spheromak. It has two oscillating injectors driven 90 deg out of phase.[23] The injectors are 180-deg segments of a toroidal pinch attached to a slotted flux conserver as shown in Fig. 11. The transformers and coils needed for the voltage and flux circuits are shown on the right. The flux conserver and injector surfaces are of high-conductivity copper alloy. The different colors are used to show electrically insulated pieces. The dashed lines on the left show the location of narrow insulating gaps or slots. These gaps allow the injector flux to oscillate in out of the injector and spheromak regions.

Because the electric field is zero in the metal of the conducting shell, the voltage across the insulating gap is uniform along its entire length. Thus, the narrow gaps in the conducting shell ensure that complete flux tubes are injected simultaneously with no open flux penetrating the wall. The transformers induce an oscillating loop voltage in each injector. The transformer cores can be small because they are driven at a high frequency. For space propulsion air core transformers might be used because of the lower mass. This transformer is the last element in the power conditioning equipment. Because this provides the current drive and the plasma ohmically heats to ignition, no significant additional mass is needed for plasma current drive and heating equipment. The toroidal flux is produced in each injector using coils, wrapped around the injectors, and by the passive, flux-shaping shells. Helicity is injected into the plasma volume at the rate $2V_{\text{inj}}\psi_{\text{inj}}$. The V_{inj} and ψ_{inj} of each injector are oscillated in phase with amplitudes ψ_0 and V_0. In one injector the flux and voltage oscillate as $\sin\omega t$, in the other as $\cos\omega t$. The helicity injection rate is $\mathrm{d}K_{\text{inj}}/\mathrm{d}t = 2V_0\psi_0\sin^2\omega t + 2V_0\psi_0\cos^2\omega t = 2V_0\psi_0 = \text{constant}$. The injectors connect to the outer fields and drive a high current density in that region. This concept is pursued at the University of Washington.[23] Figure 12 is an assembly drawing of this experiment.

C. Exhaust Divertor

In addition to the HIT-SI geometry, the fusion propulsion engine has exhaust pipes attaching to the geometric center of the bowtie spheromak. The edge flux will be diverted out the conducting pipes. Figure 13 shows a minimum energy state equilibrium calculation for a bowtie spheromak with edge field lines diverted out exhaust pipes. The liquid lithium coolant flows around the exhaust pipes as it enters and leaves the blanket around the spheromak.

To create thrust, the exhaust must be redirected in one direction so that net thrust will be realized. A conducting pipe with some parallel

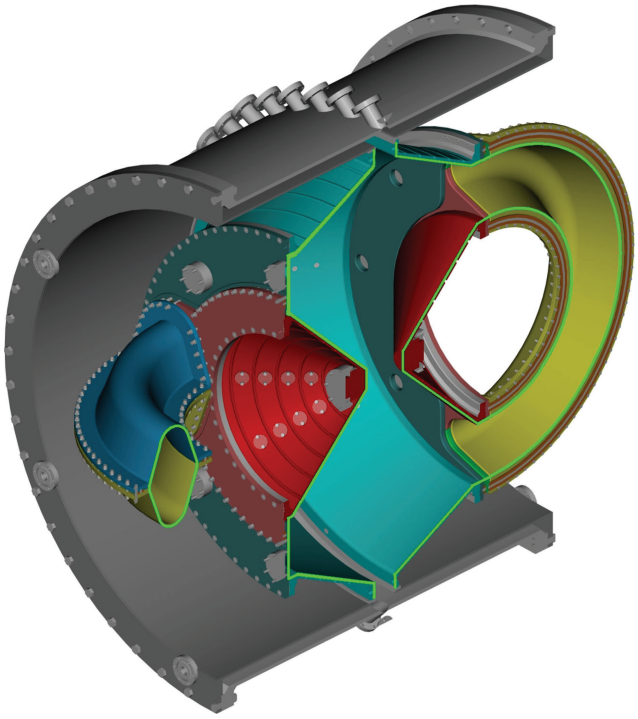

Fig. 12 Cutaway view of the HIT-SI experiment that has steady-state helicity injection current drive. All colored parts are copper; the gray is stainless steel. The light green surface is the cross-section cut on the copper.

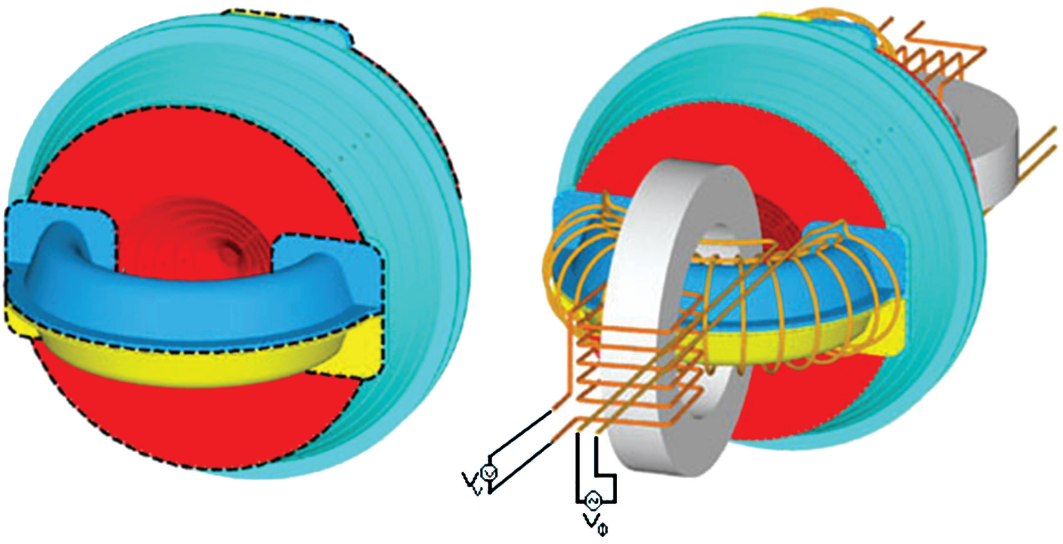

Fig. 11 First wall of HIT-SI.

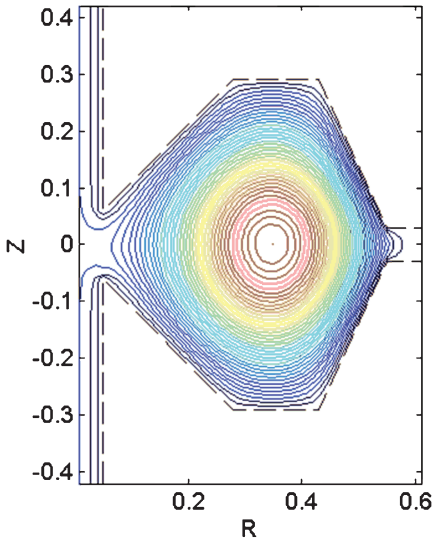

Fig. 13 Minimum energy state equilibrium calculation for a bowtie spheromak with edge field lines diverted out exhaust pipes.

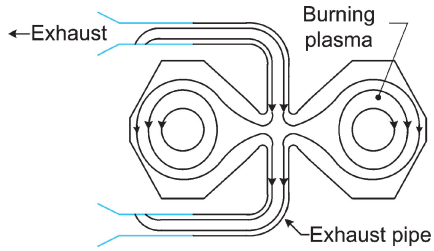

Fig. 14 Sketch of the topology of the exhaust tubes with magnetic field lines. The magnetic field lines have arrows showing the direction. Black walls are conducting. Blue walls are insulating.

magnetic field can turn a corner, and the plasma will follow the field with less than a gyro radius of motion off the field lines. The tubes or ducts maintain a magnetic field within to divert the plasma around a 90-deg corner as shown in Fig. 14. The field lines are turned into the wall at the end of the ducts using insulators; this allows the plasma to exhaust through the pipes without causing excess drag.

D. Transporting Diverted Plasma to the Exhaust

Using the generalized Hall, Ohm's law, and the magnetohydrodynamics momentum equation and neglecting ohmic heating and pressure gradient as well as gravity terms, the two equations become

$$\boldsymbol{E} + \boldsymbol{v} \times \boldsymbol{B} = \frac{(\boldsymbol{j} \times \boldsymbol{B})}{en} \tag{12}$$

$$\rho \frac{\mathrm{d}\boldsymbol{v}}{\mathrm{d}t} = \boldsymbol{j} \times \boldsymbol{B} \tag{13}$$

Because the walls of the tube are conducting, there is no potential difference across them so that $E = 0$. Substituting Eq. (12) into Eq. (13) results in the following:

$$en(\boldsymbol{v} \times \boldsymbol{B}) = \rho \frac{\mathrm{d}\boldsymbol{v}}{\mathrm{d}t} \tag{14}$$

Using this governing equation, the following description shows how the plasma turns the corner in the duct.

Figure 15 illustrates the scenario of plasma entering a turn. From the figure we see that initially, $\boldsymbol{v} \times \boldsymbol{B}$ is in the positive z direction.

From Eq. (14), $\mathrm{d}\boldsymbol{v}/\mathrm{d}t$ is in the positive z direction, and the ions begin to accelerate out of the page. This new component of velocity produces a $v_z B_\phi$, resulting in a force in the inward radial direction.

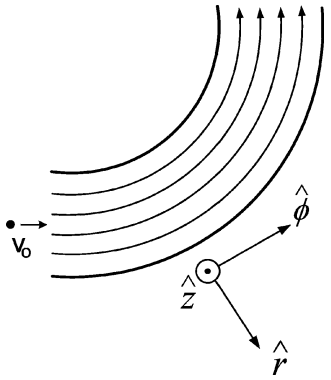

Fig. 15 Conducting copper duct with magnetic topology and geometry. The arrow shows the direction of the fluid flow and of the magnetic field. The electric field is zero because of the boundary is a conductor.

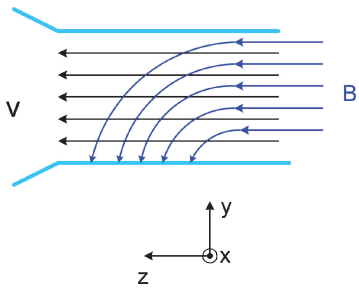

Fig. 16 Magnetic field lines diverted into wall of insulating duct at end of exhaust tube. Black lines show the plasma flow, and blue lines with arrows show the magnetic field lines.

This force increases until $\rho \mathrm{d}v_r/\mathrm{d}t = \rho v^2_{\mathrm{parallel}}/r$, which is the centripetal force necessary to keep the particles traveling in a path such that the non-z components of velocity are parallel to B_ϕ. While moving along this path, there are no other forces on the plasma (when viewed as a fluid) save the centripetal force, and so this is the equilibrium trajectory.

To see how far the ions travel in the z direction (across the field), during this quarter turn the governing equation is rearranged to give

$$env_z B = \rho\left(v^2_{\mathrm{parallel}}/r\right) \tag{15}$$

which then leads to:

$$v_z t_t = (\pi/2)(mv_{\mathrm{parallel}}/eB) = (\pi/2)r_{\mathrm{gi}} \tag{16}$$

where t_t is the time it takes for the plasma to turn 90 deg. Thus, the plasma drifts about a gyro-radius as it makes the turn, which can be quite small, and the plasma essentially follows the field lines. The key element is the conducting wall, which provides the return path for the current that traverses the plasma in the z direction. This current crossed into the guide field turns the plasma and keeps it following the field.

When the ions have reached the end of the exhaust duct, the magnetic field lines are turned into the wall as shown in Fig. 16.

The end of the duct is made of an insulating material to allow an electric field to be produced by the particle drifts in the $\pm x$ directions. An E field into the page builds up, which allows the plasma to cross the magnetic B field undeflected. From a particle viewpoint, the force caused by this electric field cancels the $\boldsymbol{v} \times \boldsymbol{B}$ force. Thus, the plasma is allowed to cross the magnetic field lines and exit the ship, producing thrust. The key elements for this concept are 1) the insulating wall so that return current cannot flow to prevent the plasma from crossing the field and 2) diverting all of the field to one side so that azimuthal currents will not flow within the plasma to prevent the plasma from crossing the B field. Simply letting the field lines symmetrically enter the insulating wall would fail because azimuthal currents would flow to prevent the plasma from crossing the field. (Another solution is to expand the duct to a large diameter at the exit. This would lower the field line tension so that it does not significantly impede the rocket and the plasma would not need to cross B-field lines.)

Figure 17 shows an artist's conception of the fusion propulsion engine. The dark blue tubes represent the inductive helicity injectors. The green pipes are the exhaust pipes for directing the diverted

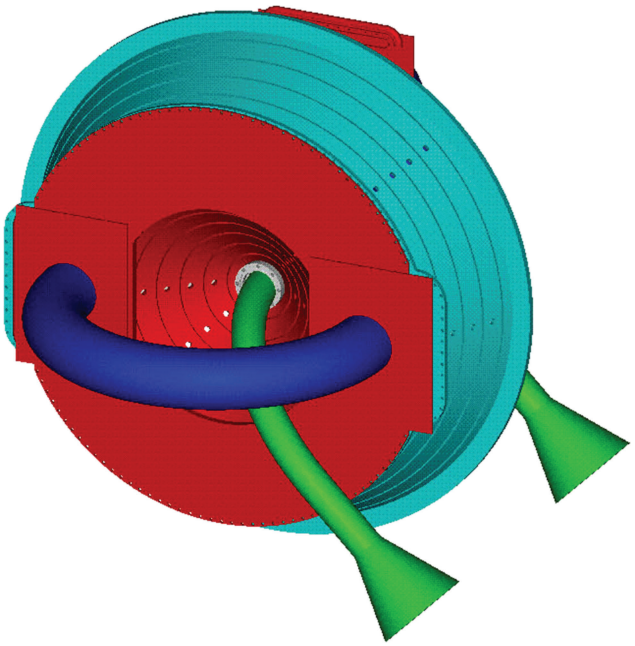

Fig. 17 Artist's conception of the first wall of a spheromak-based fusion propulsion engine.

plasma to the exhaust. The red and light blue define the first wall of the spheromak confinement region.

VII. Conclusions

The use of a fusion reactor based on the spheromak magnetic confinement device as a rocket engine for interplanetary space travel is explored. For the purposes of this study, a fairly accurate analytic expression for the minimum round-trip travel time subject to the constraints of the power-to-mass ratio and a lower bound on the exhaust velocity was derived. The power is that into the exhaust, and the mass is the total mass at the end of the mission. The diverted edge plasma from the reactor is directed into space to create the engine exhaust. This eliminates the need for divertor plates, a major problem area in controlled fusion. The edge plasma is heated from the power produced by charged fusion reaction products and electrical input power. Most of the exhaust mass is unburnt fuel. For this concept, pure deuterium is used as the fuel. Its low cross section disadvantage (compared to DT and D^3He) is offset by the abundance of the fuel, the lack of the need for breeding, and the simplicity of having the fusion fuel being identical to the inert fuel. The neutron power and other radiation power are used to generate electricity, in an optimized Brayton cycle including radiator mass in the optimization. This electricity is used to power the spacecraft and to sustain the magnetic fields of the spheromak. Although the power generator is very massive, its use avoids the need to evoke untested direct conversion schemes.

The reactor uses liquid lithium coolant and superconducting magnets. The total mass not including fuel is estimated to be 540 metric tons. This concept might achieve power to mass ratios of nearly 2 kW/kg giving round-trip times to Mars and Europa of about 100 days and 380 days respectively in a ship large enough to support human life.

The only major extrapolation from existing technology is the spheromak reactor itself. The reactor represents a large extrapolation from a small, pulsed experiment to over an order-of-magnitude larger steady-state reactor. An attractive reactor is found by assuming constant beta, constant density, constant current density, Spitzer resistivity scaling, and steady inductive helicity injection for sustainment. Work is presently underway to develop this confinement concept. If the spheromak reaches its potential as a fusion plasma confinement device, then it will lead to a most attractive space propulsion method for exploration of the solar system.

Appendix: A

The following is a more detailed derivation of Eqs. (2–4). Finding the optimum I_{SP} at any given time requires maximizing the energy efficiency by minimizing the energy required to produce the rocket exhaust. There are two energy costs to produce exhaust. The first is the internal energy spent. For δm mass exhausted, this energy is $(\frac{1}{2})(\delta m)c_e^2$. The other cost is the energy spent to bring the fuel to the speed of the rocket. This is $(\frac{1}{2})(\delta m)v^2$. The total energy required divided by the impulse is

$$\frac{W}{I} = \frac{\frac{1}{2}(\delta m)c_e^2 + \frac{1}{2}(\delta m)v^2}{(\delta m)c_e}$$

$$\frac{W}{I} = \frac{1}{2}\left(c_e + \frac{v^2}{c_e}\right) \tag{A1}$$

We find the extreme with respect to c_e by taking $\mathrm{d}(W/I)/\mathrm{d}c_e = 0$. This gives

$$\tfrac{1}{2}\left(1 - v^2/c_e^2\right) = 0, \qquad \text{or when} \qquad v = c_e \tag{A2}$$

The maximum efficiency turns out to be 100%, and it is when the exhaust speed matches the rocket speed, that is, when the exhaust is made to be at rest in the initial stationary reference frame. Thus, the I_{SP} needs to increase during the mission for maximum efficiency. Because all of the energy supplied to the exhaust ends up as kinetic energy of the final mass, this condition also represents the shortest time to reach that Δv_f, the highest Δv_f it can reach in that time, and the farthest distance it can go in that time.

When the c_e is optimized to match the rocket speed, the limiting factor is the power-to-mass ratio, where the mass is the total mass at the end of the mission and the power is that going into exhaust.

We can calculate and solve the equation of motion if we use the fact that the power is constant and the exhaust speed is the rocket speed. The constant power condition gives us

$$P = \text{constant} = \tfrac{1}{2}\dot{m}c_e^2, \qquad \dot{m} = 2P/c_e^2 \tag{A3}$$

We insert Eq. (A3) into Newton's law using $v = c_e$:

$$m\frac{\mathrm{d}v}{\mathrm{d}t} = \dot{m}v = \frac{2P}{v}, \qquad mv\frac{\mathrm{d}v}{\mathrm{d}t} = 2P \tag{A4}$$

Because the exhaust comes to rest in the initial inertial frame, the momentum in the exhaust is zero. Thus the momentum of the rocket and fuel is constant and equals, for example, the final momentum so that we have $mv = m_f \Delta v_f$. Thus we have

$$a = \frac{\mathrm{d}v}{\mathrm{d}t} = \frac{2P}{m_f \Delta v_f} \tag{A5}$$

where a is the acceleration. Thus, the acceleration depends on the power-to-mass ratio and Δv_f . The big advantage of controllable c_e is that the initial mass required does not go exponentially with the final velocity but is only proportional to the final velocity.

The rocket accelerates uniformly for the first half of the outbound flight and then slows to zero for the destination and repeats for the return flight all at the same magnitude of acceleration, yielding

$$\Delta v_f = a t_m \equiv \int |\mathrm{d}v| \tag{A6}$$

The total distance traveled is

$$\begin{aligned} Z_{\mathrm{rt}} &= 4 \times \frac{1}{2} a \left(\frac{t_m}{4}\right)^2 = \frac{1}{8} a t_m^2 \\ &= \frac{1}{8}\frac{1}{a}\Delta v_f^2 \\ &= \frac{1}{16}\frac{m_f \Delta v_f}{P}\Delta v_f^2 \\ &= \frac{1}{16}\frac{m_f}{P}\Delta v_f^3 \end{aligned} \tag{A7}$$

Using Eq. (A6) and the first line of Eq. (A7) allows us to find Δv_f as a function of t_m and $Z_{\rm rt}$. Substituting yields

$$Z_{\rm rt} = \tfrac{1}{8}(m_f/P)(8Z_{\rm rt}/t_m)^3, \qquad Z_{\rm rt}^2 = (P/32m_f)t_m^3 \tag{A8}$$

This is essentially Eq. (2).

In addition to having no energy in the exhaust, there is also no momentum in the exhaust: $m_0 v_0 = m_f \Delta v_f$. Because we must have the necessary final momentum, there must also be an initial momentum. Thus, if the initial velocity is zero the initial mass must be infinite. Neither a zero initial exhaust velocity nor an infinite initial mass are practical. In practice, there is a minimum exhaust speed $c_{\rm ex}$ for which the propulsion unit will be efficient. One solution is to keep the constant acceleration result but start with the minimum exhaust velocity $c_{\rm ex}$. (Surprisingly, this gave shorter mission times than having $c_e = c_{\rm ex}$ until $\Delta v = c_{\rm ex}$ and then have $c_e = \Delta v$ for the remainder of the trip.) This will also yield a finite initial mass. To write down the acceleration, imagine the rocket started with infinite mass and zero velocity in an inertial frame moving at $-c_{\rm ex}$ with respect to the Earth. The rocket reaches the Earth with zero velocity with respect to the Earth where our mission starts. In this case we can use Eq. (A5) for the acceleration, but the imagined mission Δv_f increases by $c_{\rm ex}$; thus, we have

$$a = \frac{2P}{m_f(\Delta v_f + c_{\rm ex})} \tag{A9}$$

Using this and Eq. (A6) and solving for a yields

$$a = \frac{-c_{\rm ex} + \sqrt{c_{\rm ex}^2 + (8P/m_f)t_m}}{2t_m} \tag{A10}$$

Substituting a from Eq. (A10) into the top Eq. (A7) and solving for P/m_f yields

$$P/m_f = 32\left(Z_{\rm rt}^2/t_m^3\right) + 4\left(c_{\rm ex}Z_{\rm rt}/t_m^2\right) \tag{A11}$$

This is essentially Eq. (3).

From the momentum being constant in the imagined frame, the mass fraction at Earth is given by

$$\frac{m_f}{m_o} = \frac{c_{\rm ex}}{c_{\rm ex} + \Delta v_f} \tag{A12}$$

If we know P/m_f, $Z_{\rm rt}$, and $c_{\rm ex}$, then Eq. (A11) can be used to find t_m. With this, the top Eq. (A7) can be used to find a and Δv_f equals at_m.

Equation (4) is an estimate of the effect that gravity might have on the mission times. It is a simple estimate. It assumes the possible additional time to change orbits caused by ignored gravity is no more than the time it takes to give the rocket the perpendicular kinetic energy equal to the change in the total orbital energy in going from Earth orbit to the destination orbit. Circular orbits are assumed. The specific potential plus kinetic energy for an object in a circular orbit around the sun are given by

$$\text{P.E.} + \text{K.E.} = -\left(v_e^2 r_e/2r\right) \tag{A13}$$

where v_e and r_e are the speed and radius of the Earth orbit and r is the radius of the object orbit. The estimated Δv^2 needed is then

$$\Delta v_{\rm PE}^2 \simeq v_e^2(1 - r_e/r_d) \tag{A14}$$

where r_d is the radius of the orbit of the destination. Using

$$Z_{\rm rt} = 2(r_d - r_e) \tag{A15}$$

yields

$$\Delta v_{\rm PE} = v_e\left(\frac{Z_{\rm rt}}{Z_{\rm rt} + 2r_e}\right)^{\frac{1}{2}} \tag{A16}$$

For simplicity we approximate the acceleration as Eq. (A5) and use Eq. (A6) to eliminate Δv_f to arrive at

$$a = (2P/m_f t_m)^{\frac{1}{2}} \tag{A17}$$

Using $t_{\rm PE} = \Delta v_{\rm PE}/a$ and Eqs. (A16) and (A17) yields

$$t_{\rm PE} = \left(\frac{Z_{\rm rt}}{Z_{\rm rt} + 2r_e}\frac{m_f t_m}{2P}\right)^{\frac{1}{2}} \tag{A18}$$

This is Eq. (4).

Expressions for trip times as a function of specific power, with both constant and variable $I_{\rm SP}$, and under a variety of other optimization constraints can be found in Ref. 24.

References

[1] Williams, C. H., Borowski, S. K., Dudzinski, L. A., and Juhasz, A. J., "A Spherical Torus Nuclear Fusion Reactor Space Propulsion Vehicle Concept for Fast Interplanetary Piloted and Robotic Missions," AIAA Paper 99-2704, 1999.

[2] Kammash, T., (ed.), *Fusion Energy in Space Propulsion*, AIAA, Washington, DC, 1995.

[3] Jarboe, T. R., Wysocki, F. J., Fernandez, J. C., Henins, I., and Marklin, G. J., "Progress with Energy Confinement Time in the CTX Spheromak," *Physics of Fluids B*, Vol. 2, 1990, p. 1342.

[4] Jahn, R. G., *Physics of Electric Propulsion*, McGraw–Hill, New York, 1968.

[5] Bate, R., Mueller, D., and White, J., *Fundamentals of Astrodynamics*, Dover, New York, 1971.

[6] Borowski, S., Dudzinski, L., and McGuire, M., "Bimodal Nulear Thermal Rocket (NTR) Propulsion for Power Rich, Artificial Gravity Human Exploration Mission to Mars," International Astronautical Federation, IAA-01-IAA.13.3.05, Oct. 2001.

[7] Hagenson, R. L., and Krakowski, R. A., "Steady-State Spheromak Reactor Studies," *Fusion Technology*, Vol. 8, 1985, p. 1606.

[8] Williams, C. H., "An Analytic Approximation to Very High Specific Impulse and Specific Power Interplanetary Space Mission Analysis," NASA TM 107058, Sept. 1995.

[9] Wysocki, F. J., Fernandez, J. C., Henins, I., Jarboe, T. R., and Marklin, G. J., "Evidence for Pressure-Driven Instability in the CTX Spheromak," *Physical Review Letters*, Vol. 61, 1988, p. 2457.

[10] Bekefi, G., *Radiation Processes in Plasmas*, Wiley, New York, 1966, Chap. 6.

[11] Zhang, Y., et al., "Recent Development of Niobium-Tin Superconducting Wire at OST," *IEEE Transactions on Applied Superconductivity*, Vol. 9, 1999, p. 1444.

[12] Shleicher, R., Raffray, A. R., and Wong, C. P., "An Assessment of the Brayton Cycle for High Performance Power Plant," *Fusion Technology*, Vol. 39, March 2001, pp. 823–827.

[13] Decher, R., *Energy Conversion*, Oxford Univ. Press, New York, 1994.

[14] Shumlak, U., and Jarboe, T. R., "Stable High Beta Spheromak Equilibria Using Concave Flux Conserver," *Physics of Plasma*, Vol. 7, 2000, p. 2959.

[15] Jarboe, T. R., "Review of Spheromak Research," *Plasma Physics and Controlled Fusion*, Vol. 36, 1994, p. 945.

[16] Taylor, J. B., "Relaxation and Magnetic Reconnection in Plasma," *Reviews of Modern Physics*, Vol. 58, 1986, p. 741.

[17] Edenstrasser, J. W., and Kassab, M. M. M., "The Plasma Transport Equations Derived by Multiple Time-Scale Expansions. II. An Application," *Physics of Plasmas*, Vol. 2, 1995, p. 1206.

[18] Woltjer, L., "A Theorem on Force-Free Magnetic Field," *Proceedings of the National Academy of Science*, Vol. 44, 1958, p. 489.

[19] Jarboe, T. R., and Alper, B., "A Model for the Loop Voltage of Reversed Field Pinches," *Physics of Fluids*, Vol. 30, 1987, p. 1177.

[20] Fernández, J. C., Bames, C. W., Jarboe, T. R., Henins, I., Hoida, H. W., Klingner, P. L., Knox, S. O., Marklin, G. J., and Wright, B. L., "Energy Confinement Studies in Spheromaks with Mesh Flux Conservers," *Nuclear Fusion*, Vol. 28, 1988, p. 1555.

[21] Moffat, H. K., *Magnetic Field Generation in Electrically Conducting Fluids*, Cambridge Univ. Press, New York, 1978.

[22] Jensen, T. H., and Chu, M. S., "The Bumpy Z-Pinch," *Journal of Plasma Physics*, Vol. 25, 1981, p. 459.

[23] Jarboe, T. R., "Steady Inductive Helicity Injection and its Application to a High-Beta Spheromak," *Fusion Technology*, Vol. 36, 1999, p. 85.

[24] Stuhlinger, E., *Ion Propulsion for Space Flight*, McGraw–Hill, New York, 1964, Chap. 4.